Functorial Krump: A Dagger-Compact Frobenius Calculus and Dual-Channel Quantum Semantics for Multi-Track Street Dance Choreography

Arun Nadarasa
Angels of Krump Movement Federation
https://arunnadarasa.github.io/quantumkrump/

Dakota Simao
Twin Bad Liks / Jr Outrage
Artistic Director & Choreographer, Geneva
https://www.youtube.com/@dakotasimao

November 2026 *Standalone Applied Category Theory Preprint*

Abstract

Formalizing dance choreography purely through directed posture graphs restricts composition to sequential, single-dancer trajectories, leaving concurrent partner duets, spatial crossovers, collective ensemble amplification, and continuous dynamic Effort modulation outside the algebraic syntax. Drawing on Categorical Quantum Mechanics and compositional distributional models (DisCoCat), we construct a two-tier categorical semantics for South Central Los Angeles Krump street dance and Laban Movement Analysis (LMA). At the solo level, we define the free category CatKS generated by six level-tagged Krump forms and seven studio transitions together with beat-counting endomorphisms, prove chronological trace factorization across round-indexed performance functors $F_r : \mathrm{CatKS} \to \mathrm{CatKP}$, and show via quiver adjacency powers that truncated Yoneda presheaf profiles $(|\mathrm{Hom}_{\leq 4}(X, A)|)_{X \in V}$ uniquely distinguish all six foundational postures. Via categorical delooping, we then lift movement generators to 1-morphisms of a parameterized symmetric monoidal †-compact category $\mathcal{C}_{\mathrm{Krump}}(\Theta)$ equipped with a special commutative †-Frobenius algebra on self-dual dancer wires D. Machine-checked rewriting in `DisCoPy 1.2.2` verifies exhaustive bifunctorial interchange confluence across all $6^4 = 1{,}296$ two-dancer two-step phrases, left/right snake yanking, involutive stage swaps, three-dancer Yang–Baxter braid coherence, and Frobenius spider fusion. Mapping $\mathcal{C}_{\mathrm{Krump}}(\Theta) \to \mathbf{FHilb}$ (strictly on orthonormal spiders and projectively on unit-norm quantum circuits), we prove a *Dual-Channel Effort Demultiplexing Theorem* for a five-stage entangled duet modulated by continuous Laban Effort parameters $(\theta, \varphi) \in [0, 2\pi)^2$: prior to the terminal climax cup ϵ_D, the two-qubit state retains unit Wootters concurrence ($\mathcal{C} \equiv 1$), maximally mixed local marginals ($\rho_A = \rho_B = \frac{1}{2} I_2$), and exact additive Stabilizer 2-Rényi Magic $M_2(\theta, \varphi) = -\log_2(1 - \frac{1}{4}\sin^2 2\theta) - \log_2(1 - \frac{1}{4}\sin^2 2\varphi)$ peaking at $\log_2(16/9) \approx 0.8301$ bits at non-Clifford quarter-turn Effort angles; upon joint Bell readout ϵ_D, Born probabilities factorize cleanly into independent product channels $P(m_0, m_1 \mid \theta, \varphi) = p_\varphi(m_0)\, p_\theta(m_1)$ saturating the multiparameter Quantum Cramér–Rao bound $I_C(\theta, \varphi) = \mathrm{diag}(1, 1)$. Finally, we formalize collision- and swap-free planar realization of symmetric monoidal crossovers $\sigma_{D,D}$ via exact Rosenberg HUBO-to-QUBO quadratization, cross-validate symbolic derivations against `pytket 2.18.1` native trapped-ion compilation and Quantinuum `Helios-1E-lite` emulator receipts (99.41% Clifford-anchor fidelity; 0 physical QPU shots), and report exact microsecond classical tensor-contraction floors ($0.63\,\mu$s).

1 Introduction

A central program of applied category theory is to equip structured human processes—natural language grammar [1], musical counterpoint and formal aesthetics [2–5], orchestral gesture [6, 7], and

discrete combinatorial reasoning [8, 9]—with compositional string-diagrammatic calculi [10] that admit functorial interpretation in finite-dimensional Hilbert spaces (**FHilb**) [11–13]. In movement and dance studies, computational formalisms have historically represented solo choreography as paths or Markov transitions on a finite posture graph. While directed quivers capture sequential grammar along a single dancer's timeline, they lack horizontal tensor product structure: two partners performing simultaneous counterpoint, crossing stage tracks without collision, establishing non-visual mutual responsiveness, or amplifying energy across a surrounding session circle cannot be expressed natively as arrows of a multi-posture quiver without an exponential Cartesian state-space blowup.

In this paper, we develop a self-contained categorical and operator-algebraic calculus for **Krump**, the expressive urban street dance created in South Central Los Angeles in the early 2000s by Ceasare "Tight Eyez" Willis, Jo'Artis "Big Mijo" Ratti, Marquisa "Miss Prissy" Gardner, Christopher "Lil C" Toler, and Jason "Slayer" Green [14], paired with Rudolf Laban and F. C. Lawrence's dynamical taxonomy of human *Effort* [15, 16]. Krump is uniquely suited to monoidal process theory for three structural reasons:

1. **Discrete Foundational Generators across Kinespheric Levels:** Its core movement vocabulary decomposes into percussive/rotational generators—`STOMP`, `JAB`, `CHEST POP`, `ARM SWING`, `BUCK HOP`, and terminal `KILL-OFF`—executed across three ordered vertical posture zones (`LIVE`, `KRUMP`, and `BUCK`).

2. **Continuous Laban Effort Modulation:** Each generator admits continuous kinematic modulation along Laban's polar Effort axes (*Weight*, *Time*, *Space*, and *Flow*), naturally parameterizing continuous unitary rotation families in SU(2).

3. **Relational Session Topology:** Authentic Krump takes place inside a communal *Session* (the traditional South Central LA circle formation), governed by non-verbal dyadic call-and-response, stage crossovers, and collective *hype* branching and convergence.

Scope and Epistemic Demarcation. Unlike broader educational or robotic companion works [17, 18], the present article focuses *exclusively* on mathematical formalization, rewrite coherence, exact operator-algebraic semantics, and verifiable circuit compilation. Two explicit boundaries govern every result below: (i) the functor $\mathcal{F}_{\theta,\varphi} : \mathcal{C}_{\mathrm{Krump}}(\Theta) \to \mathbf{FHilb}$ is a *formal structural homomorphism* between a choreographic process theory and finite-dimensional quantum linear algebra—macroscopic human bodies experience zero biological quantum coherence; and (ii) two- to four-qubit choreographic circuits contract classically on a single CPU core in 0.63–1.74 μs, so quantum compilation targets compositional semantics, stabilizer/magic characterization, and noise-model benchmarking rather than computational speedup over classical linear algebra.

Summary of Contributions.

- **Solo Quiver Categories and Finite Yoneda Distinguishability (Section 2):** We formalize the level-tagged solo posture quiver CatKS, separate zero-duration groove identities id_A from beat-counting endomorphisms $r_A \in (\mathbb{N}, +, 0)$, prove round-indexed performance factorization $F_r \circ P : [m] \to \mathrm{CatKP}$ (Proposition 2.3), and prove that truncated incoming path-count vectors of length ≤ 4 uniquely identify every Krump posture under the Yoneda embedding (Theorem 2.4).

- **Delooped †-Compact Frobenius Choreography Calculus (Section 3):** Passing via categorical delooping to a single self-dual dancer object D, we present the parameterized symmetric monoidal †-compact Frobenius category $\mathcal{C}_{\mathrm{Krump}}(\Theta)$ and verify normal-form confluence across all 1,296 two-step duet phrases, snake equations, three-dancer Yang–Baxter braid coherence, and Frobenius session-hype fusion in `DisCoPy 1.2.2` [19] (Theorem 3.2).

- **Strict vs. Projective Semantics & Dual-Channel Effort Demultiplexing (Section 4):** After reconciling strict orthonormal-spider semantics in **FHilb** with unit-norm circuit post-selection in **PFHilb** (Theorem 4.1) and establishing an antisymmetric Bell ricochet lemma (Lemma 4.2), we prove our central analytical result (Theorem 4.3): in the five-stage parameterized duet $\mathcal{D}(\theta, \varphi)$, local single-dancer measurements yield zero Fisher information ($\rho_A = \rho_B = \frac{1}{2} I_2$), Stabilizer 2-Rényi Magic [20] decomposes additively across the two dancers' Effort parameters up to $\log_2(16/9) \approx 0.8301$ bits, and joint climax-cup Bell readout factorizes into exact independent marginals $P(m_0, m_1 \mid \theta, \varphi) = p_\varphi(m_0)\, p_\theta(m_1)$ achieving diagonal Fisher information $I_C(\theta, \varphi) = \mathrm{diag}(1, 1)$.
- **Planar Stage Realizability & Multi-Backend Verification (Sections 5–6):** We prove exactness of Rosenberg HUBO-to-QUBO quadratization [21] for vertex- and swap-free realization of $\sigma_{D,D}$ on discrete stage graphs (Proposition 5.1) and validate all symbolic predictions against `SymPy 1.14.0`, `DisCoPy 1.2.2`, `pytket 2.18.1` [22] trapped-ion gate rebasing, and Quantinuum `Helios-1E-lite` noisy emulator receipts.

2 Biomechanical Frame, Solo Quivers, and Finite Yoneda Profiles

2.1 Stage-Fixed Anatomical Kinesphere Frame

To ensure that geometric coordinates assigned to bodily postures are biomechanically unambiguous, we fix a right-handed Cartesian kinesphere frame $(\hat{x}_{\text{forward}}, \hat{y}_{\text{left}}, \hat{z}_{\text{up}})$ satisfying $\hat{x}_{\text{forward}} \times \hat{y}_{\text{left}} = \hat{z}_{\text{up}}$ anchored at the dancer's anatomical center of mass (navel / lumbar L3 vertebra) in neutral mid-level `KRUMP` stance ($\theta = \pi/2$). Rather than requiring the head or torso to invert below the floor plane, polar colatitude $\theta \in [0, \pi]$ maps affinely onto physiological center-of-mass elevation $h(\theta) \in [h_{\min}, h_{\max}]$:

$$h(\theta) = h_{\min} + \frac{h_{\max} - h_{\min}}{2}\,(1 + \cos\theta), \tag{1}$$

identifying $+Z$ ($\theta = 0 \mapsto |0\rangle$) with upright `LIVE` extension ($h = h_{\max}$), the equatorial horizon ($\theta = \pi/2 \mapsto (|0\rangle + e^{i\varphi}|1\rangle)/\sqrt{2}$) with mid-level `KRUMP` stance, and $-Z$ ($\theta = \pi \mapsto |1\rangle$) with a deep knee-flexed `BUCK` crouch ($h = h_{\min}$). Azimuthal angle $\varphi \in [0, 2\pi)$ is referenced to the *stage-fixed* downstage vector $\hat{x}_{\text{forward}}$ ($\varphi = 0$ downstage, $\varphi = \pi/2$ stage-left, $\varphi = \pi$ upstage, $\varphi = 3\pi/2$ stage-right), decoupling horizontal strike direction φ from local pelvic yaw.

Table 1: Three-way correspondence between Laban Effort polarities, Krump studio foundations, and SU(2)/projective operators on $\mathbb{C}^2$.

Generator	Level	Primary Laban Effort	Anchor	Continuous Effort Family
`STOMP`	`BUCK`	Strong · Sudden · Direct	H	Hadamard superposition launch
`JAB`	`LIVE`	Light/Strong · Sudden · Direct	X	$R_x(\pi)$ bit-flip strike (up to $-i$)
`CHEST POP`	`KRUMP`	Strong · Sudden · Bound	Z	$R_z(\pi)$ thoracic phase inversion
`ARM SWING`(θ)	`KRUMP`	Strong · Sustained · Indirect	$R_x(\pi/2)$	$R_x(\theta) = \exp(-i\frac{\theta}{2}X)$, $\theta \in [0, 2\pi)$
`BUCK HOP`(φ)	`BUCK`	Strong · Sudden · Free	$S \equiv R_z(\pi/2)$	$R_z(\varphi) = \exp(-i\frac{\varphi}{2}Z)$, $\varphi \in [0, 2\pi)$
`KILL-OFF`	`BUCK`	Strong · Sudden · Bound	$P_0 = \|0\rangle\langle 0\|$	Terminal Hermitian idempotent projector

2.2 The Free Category CatKS and Chronological Performance Traces

Following Khan's categorical formalization of Hanslick's musical aesthetics [4, 23] and Mazzola–Mannone hypergestures [2], we first formalize solo sequential Krump syntax.

Definition 2.1 (Category of Solo Krump Structures CatKS)**.** Let $\mathcal{G} = (V, E)$ be the finite directed quiver with six level-tagged posture vertices

$$V = \big\{\texttt{STOMP}_{\text{BUCK}},\ \texttt{CHEST POP}_{\text{KRUMP}},\ \texttt{JAB}_{\text{LIVE}},\ \texttt{ARM SWING}_{\text{KRUMP}},\ \texttt{BUCK HOP}_{\text{BUCK}},\ \texttt{KILL-OFF}_{\text{BUCK}}\big\} \tag{2}$$

and seven canonical generating transition edges $E = \{f, g, h, j, k, l, m\}$:

$$\begin{aligned} f &: \texttt{STOMP}_{\text{BUCK}} \to \texttt{CHEST POP}_{\text{KRUMP}}, & g &: \texttt{CHEST POP}_{\text{KRUMP}} \to \texttt{JAB}_{\text{LIVE}}, \\ h &: \texttt{JAB}_{\text{LIVE}} \to \texttt{KILL-OFF}_{\text{BUCK}}, & j &: \texttt{ARM SWING}_{\text{KRUMP}} \to \texttt{CHEST POP}_{\text{KRUMP}}, \\ k &: \texttt{BUCK HOP}_{\text{BUCK}} \to \texttt{CHEST POP}_{\text{KRUMP}}, & l &: \texttt{STOMP}_{\text{BUCK}} \to \texttt{ARM SWING}_{\text{KRUMP}}, \\ m &: \texttt{CHEST POP}_{\text{KRUMP}} \to \texttt{ARM SWING}_{\text{KRUMP}}. \end{aligned}$$

Let $\mathcal{G}' = (V, E \cup \{r_A : A \to A\}_{A \in V})$ adjoin a generating repetition self-loop r_A at each vertex $A \in V$. The *Category of Solo Krump Structures* is the free category $\mathrm{CatKS} := \mathrm{Free}(\mathcal{G}')$.

Remark 2.2 (Zero-Beat Groove Identity vs. Discrete Beat Monoids)**.** In CatKS, the categorical identity $\mathrm{id}_A : A \to A$ is the empty path of beat length 0, modeling continuous maintenance of baseline postural *groove* without initiating a new count ($\mathrm{id}_A \circ \mathrm{id}_A = \mathrm{id}_A$). Conversely, the powers $\{r_A^k\}_{k \in \mathbb{N}}$ of the generating self-loop r_A generate a free monoid $\mathrm{End}_{\mathrm{rep}}(A) \cong (\mathbb{N}, +, 0)$ recording k discrete musical beat strikes at posture A. Defining beat duration $\ell : \mathrm{Mor}(\mathrm{CatKS}) \to \mathbb{N}$ on generators by $\ell(e) = 1$ for all $e \in E \cup \{r_A\}_{A \in V}$ and $\ell(\mathrm{id}_A) = 0$ yields a strict functor $\ell : \mathrm{CatKS} \to \mathbf{B}\mathbb{N}$ into the single-object delooping of $(\mathbb{N}, +, 0)$.

In a multi-round Krump battle ($r \in \{1, 2, 3\}$), a dancer revisits the same structural posture $A \in V$ multiple times within a single round with escalating dramatic context. Modeling performance directly as a naive map $V \to \mathrm{Events}$ would violate single-valuedness on objects. Let $[m] := (0 \leq 1 \leq \cdots \leq m)$ denote the finite ordinal poset category of m chronological musical counts.

Proposition 2.3 (Chronological Battle Factorization)**.** *Let* CatKP *be the category whose objects are round-indexed performative state classes* $(r, [A]_{\mathrm{perf}})$ *and whose morphisms are performed studio transitions within Round* r*. For each round* $r \in \{1, 2, 3\}$*, the assignment* $F_r(A) = (r, [A]_{\mathrm{perf}})$ *on* V *and* $F_r(e) = e_{\mathrm{perf},r}$ *on* $E \cup \{r_A\}_{A \in V}$ *extends uniquely to a strict functor* $F_r : \mathrm{CatKS} \to \mathrm{CatKP}$*. Moreover, any* m*-beat solo phrase revisiting vertices arbitrarily is uniquely represented as an ordinal path functor* $P : [m] \to \mathrm{CatKS}$ *whose performed chronological trace is the composite functor* $T_r := F_r \circ P : [m] \to \mathrm{CatKP}$*.*

Proof. By the universal property of the free category $\mathrm{CatKS} = \mathrm{Free}(\mathcal{G}')$ ($\mathrm{Free} \dashv U : \mathbf{Cat} \to \mathbf{Quiv}$), any quiver homomorphism $\mathcal{G}' \to U(\mathrm{CatKP})$ extends uniquely to a functor $F_r : \mathrm{CatKS} \to \mathrm{CatKP}$ preserving identity paths $F_r(\mathrm{id}_A) = \mathrm{id}_{F_r(A)}$ and path concatenation $F_r(p_2 \circ p_1) = F_r(p_2) \circ F_r(p_1)$. Similarly, $[m] = \mathrm{Free}(0 \to 1 \to \cdots \to m)$, so specifying a sequence of m composable edges $(e_1, \ldots, e_m)$ in $\mathcal{G}'$ defines a unique functor $P : [m] \to \mathrm{CatKS}$ with $P(i-1 \leq i) = e_i$. Since functors compose associatively in $\mathbf{Cat}$, $T_r = F_r \circ P$ assigns distinct chronological indices $i \neq j \in [m]$ to distinct time steps while preserving strict single-valuedness of F_r on $\mathrm{Ob}(\mathrm{CatKS})$. □

2.3 Yoneda Presheaf Profiles on CatKS

By the Yoneda Lemma [24], the Yoneda embedding $Y : \mathrm{CatKS} \hookrightarrow [\mathrm{CatKS}^{\mathrm{op}}, \mathbf{Set}]$, $A \mapsto \mathrm{Hom}_{\mathrm{CatKS}}(-, A)$, is full and faithful: a Krump posture A is determined up to unique isomorphism by the contravariant presheaf of all incoming transitions terminating at A. Because CatKS contains the directed 2-cycle $\texttt{CHEST POP}_{\text{KRUMP}} \underset{j}{\overset{m}{\rightleftarrows}} \texttt{ARM SWING}_{\text{KRUMP}}$, full Hom-sets are countably infinite; however, finite-horizon path counts already provide a complete combinatorial invariant.

Theorem 2.4 (Finite-Horizon Yoneda Profile Distinguishability)**.** *Let $A_{\mathcal{G}} \in \{0,1\}^{6\times 6}$ be the transition adjacency matrix of $\mathcal{G} = (V, E)$ ordered as in* (2)*, and for $L \in \mathbb{N}$ define the truncated incoming path-count matrix $M_{\leq L} := \sum_{k=0}^{L} A_{\mathcal{G}}^k$, whose (X, A)-entry equals the number of repetition-free morphisms in* CatKS *from X to A of length at most L. Then:*

1. *Already at horizon $L = 1$ (and for every $L \geq 1$), the six column vectors $\{M_{\leq L}(-, A)\}_{A\in V}$ are pairwise distinct.*

2. *At four-beat musical bar horizon $L = 4$, $\texttt{CHEST POP}_{\mathrm{KRUMP}}$ and $\texttt{ARM SWING}_{\mathrm{KRUMP}}$ act as the relational hubs of* CatKS *with $\sum_{X\in V} M_{\leq 4}(X, \texttt{CHEST POP}_{\mathrm{KRUMP}}) = 11$ repetition-free incoming paths (72 incoming paths when including beat-repetition endomorphisms r_X, strictly maximizing over V), whereas $\texttt{KILL-OFF}_{\mathrm{BUCK}}$ is strictly terminal-absorbing ($\mathrm{Hom}_{\mathrm{CatKS}}(\texttt{KILL-OFF}_{\mathrm{BUCK}}, B) = \emptyset$ for all $B \neq \texttt{KILL-OFF}_{\mathrm{BUCK}}$).*

Proof. Direct evaluation of $M_{\leq 4} = I_6 + A_{\mathcal{G}} + A_{\mathcal{G}}^2 + A_{\mathcal{G}}^3 + A_{\mathcal{G}}^4$ yields the exact integer matrix in Table 2. Already at $L = 1$, $I_6 + A_{\mathcal{G}}$ has six distinct columns because incoming neighborhoods $N^-(A) \cup \{A\}$ differ pairwise across V. Summing column 2 of $M_{\leq 4}$ gives $4+3+0+2+2+0 = 11$ repetition-free paths and $\sum_{X\in V}(\sum_{k=0}^{4}(I_6 + A_{\mathcal{G}})^k)_{X,2} = 26+16+0+15+15+0 = 72$ extended paths (exceeding $\texttt{ARM SWING}_{\mathrm{KRUMP}}$ at 68; Table 2). Row 6 of $A_{\mathcal{G}}$ is identically zero, so $(A_{\mathcal{G}}^k)_{6,B} = 0$ for all $k \geq 1$ and $B \in V$, leaving only powers of $r_{\texttt{KILL-OFF}}$ at $B = \texttt{KILL-OFF}_{\mathrm{BUCK}}$. □

Table 2: Exact truncated Yoneda path-count matrix $M_{\leq 4}(X, A) = \sum_{k=0}^{4}(A_{\mathcal{G}}^k)_{X,A}$ across one 4-beat bar in CatKS (parentheses in bottom row denote extended counts under $I_6 + A_{\mathcal{G}}$ including self-loops r_X).

Source $X \setminus$ **Target** A	STOMP	CHEST POP	JAB	ARM SWING	BUCK HOP	KILL-OFF
$\texttt{STOMP}_{\mathrm{BUCK}}$	1	4	3	4	0	2
$\texttt{CHEST POP}_{\mathrm{KRUMP}}$	0	3	2	2	0	2
$\texttt{JAB}_{\mathrm{LIVE}}$	0	0	1	0	0	1
$\texttt{ARM SWING}_{\mathrm{KRUMP}}$	0	2	2	3	0	1
$\texttt{BUCK HOP}_{\mathrm{BUCK}}$	0	2	2	2	1	1
$\texttt{KILL-OFF}_{\mathrm{BUCK}}$	0	0	0	0	0	1
Total Incoming $\sum_X M_{\leq 4}(X, A)$	**1** (5)	**11** (72)	**10** (58)	**11** (68)	**1** (5)	**8** (42)

3 Categorical Delooping: The Dagger-Compact Frobenius Calculus $\mathcal{C}_{\mathrm{Krump}}(\Theta)$

To compose multiple dancers concurrently in space, we apply a process-theoretic delooping lift: rather than encoding postures as objects and solo transitions as 1-morphisms, we introduce a single generating object D representing a persistent *dancer state track* and promote Krump movements to 1-morphisms $D \to D$. Parallel duet and ensemble formations then arise natively as monoidal tensor powers $D^{\otimes n}$.

Definition 3.1 (Parameterized Choreographic Category $\mathcal{C}_{\mathrm{Krump}}(\Theta)$)**.** Let $\Theta = [0, 2\pi)$ denote the Effort parameter circle. We define $(\mathcal{C}_{\mathrm{Krump}}(\Theta), \otimes, I, \sigma, \dagger)$ as the free symmetric monoidal †-category [11, 13] generated by a single self-dual object D ($D^* = D$) equipped with:

1. **Choreographic Box Signature $\Sigma_{\mathrm{Krump}}(\Theta)$:** Discrete involutive/Hermitian generators $\texttt{STOMP}, \texttt{JAB}, \texttt{CHEST POP}, \texttt{KILL-OFF} : D \to D$ (with $g^\dagger = g$) together with two continuous Effort-indexed rotation families $\texttt{ARM SWING}(\theta) : D \to D$ and $\texttt{BUCK HOP}(\varphi) : D \to D$ ($\theta, \varphi \in \Theta$) satisfying groupoid/group laws $\texttt{ARM SWING}(0) = \mathrm{id}_D$, $\texttt{ARM SWING}(\theta_2) \circ$

`ARM SWING`$(\theta_1) =$ `ARM SWING`$(\theta_1 + \theta_2 \bmod 2\pi)$, `ARM SWING`$(\theta)^\dagger =$ `ARM SWING`$(-\theta)$, and analogously for `BUCK HOP`(φ). The discrete studio anchor subcategory $\mathcal{C}_{\mathrm{Krump}} \subset \mathcal{C}_{\mathrm{Krump}}(\Theta)$ fixes $\theta = \varphi = \pi/2$.

2. **Special Commutative †-Frobenius Algebra on D [12]:** Morphisms $\delta : D \to D \otimes D$ (*hype split*), $\mu = \delta^\dagger : D \otimes D \to D$ (*hype merge*), $\iota : I \to D$ (*neutral entry*), and $\zeta = \iota^\dagger : D \to I$ (*neutral exit*) satisfying coassociativity, cocommutativity ($\sigma_{D,D} \circ \delta = \delta$), counit $(\zeta \otimes \mathrm{id}_D) \circ \delta = \mathrm{id}_D$, the Frobenius law

$$(\mathrm{id}_D \otimes \mu) \circ (\delta \otimes \mathrm{id}_D) = \delta \circ \mu = (\mu \otimes \mathrm{id}_D) \circ (\mathrm{id}_D \otimes \delta), \tag{3}$$

and specialness $\mu \circ \delta = \mathrm{id}_D$.

3. **Induced †-Compact Duality [11]:** The entanglement cap $\eta_D := \delta \circ \iota : I \to D \otimes D$ and climax cup $\epsilon_D := \zeta \circ \mu = \eta_D^\dagger : D \otimes D \to I$.

Theorem 3.2 (Diagrammatic Coherence, Braid Involution, and Spider Fusion in $\mathcal{C}_{\mathrm{Krump}}$)**.** *In $\mathcal{C}_{\mathrm{Krump}}(\Theta)$ (and concretely within the free Frobenius hypergraph calculus of `DisCoPy 1.2.2` [19]):*

1. ***Bifunctorial Interchange Confluence:*** *For every choice of four movement generators $f_1, f_2, g_1, g_2 \in \Sigma_{\mathrm{Krump}}$, sequential-then-parallel phrasing $(f_2 \circ f_1) \otimes (g_2 \circ g_1)$ and synchronized beat-layer phrasing $(f_2 \otimes g_2) \circ (f_1 \otimes g_1)$ reduce under `normal_form()` to the identical canonical normal form (*1,296/1,296 *exhaustive 4-tuples verified).*

2. ***Dagger-Compact Snake Coherence:*** *Both yanking identities hold strictly:*

$$(\epsilon_D \otimes \mathrm{id}_D) \circ (\mathrm{id}_D \otimes \eta_D) = \mathrm{id}_D = (\mathrm{id}_D \otimes \epsilon_D) \circ (\eta_D \otimes \mathrm{id}_D). \tag{4}$$

3. ***Symmetric Three-Dancer Crossover Coherence:*** *Stage crossover $\sigma_{D,D} : D \otimes D \to D \otimes D$ is involutive ($\sigma_{D,D} \circ \sigma_{D,D} = \mathrm{id}_{D \otimes D}$) and satisfies the three-strand Yang–Baxter / symmetric-group relation on $D^{\otimes 3}$:*

$$(\sigma_{D,D} \otimes \mathrm{id}_D) \circ (\mathrm{id}_D \otimes \sigma_{D,D}) \circ (\sigma_{D,D} \otimes \mathrm{id}_D) = (\mathrm{id}_D \otimes \sigma_{D,D}) \circ (\sigma_{D,D} \otimes \mathrm{id}_D) \circ (\mathrm{id}_D \otimes \sigma_{D,D}). \tag{5}$$

4. ***Session Hype Spider Normal Form:*** *Every connected acyclic or cyclic network built from $\delta, \mu, \iota, \zeta, \sigma_{D,D}, \eta_D, \epsilon_D$ with m input dancer tracks and k output dancer tracks fuses uniquely to the canonical Frobenius spider $S_{m,k} : D^{\otimes m} \to D^{\otimes k}$.*

Proof. Part (1) follows from the Eckmann–Hilton / Joyal–Street planar isotopy theorem for monoidal categories [10], implemented constructively via interchanger left-leaning topological sort in `DisCoPy`'s `Diagram.normal_form()`, which we additionally checked exhaustively over all $6^4 = 1{,}296$ generator tuples. For Part (2), substituting $\eta_D = \delta \circ \iota$ and $\epsilon_D = \zeta \circ \mu$ gives

$$\begin{aligned}(\epsilon_D \otimes \mathrm{id}_D) \circ (\mathrm{id}_D \otimes \eta_D) &= (\zeta \otimes \mathrm{id}_D) \circ (\mu \otimes \mathrm{id}_D) \circ (\mathrm{id}_D \otimes \delta) \circ (\mathrm{id}_D \otimes \iota) \\ &\overset{(3)}{=} (\zeta \otimes \mathrm{id}_D) \circ \delta \circ \mu \circ (\mathrm{id}_D \otimes \iota) = \mathrm{id}_D \circ \mathrm{id}_D = \mathrm{id}_D,\end{aligned}$$

and symmetrically for the right snake. Part (3) holds because $\mathcal{C}_{\mathrm{Krump}}(\Theta)$ is symmetric monoidal, so wiring permutations factor through the symmetric group S_n (verified via cospan hypergraph isomorphism `to_hypergraph()` on $D^{\otimes 2}$ and $D^{\otimes 3}$). Part (4) is the Spider Theorem for special commutative †-Frobenius algebras [12, 13]: connectedness collapses internal loops via $\mu \circ \delta = \mathrm{id}_D$, while associativity, commutativity, and the Frobenius law (3) eliminate tree topology dependence, leaving only boundary arities (m, k). □

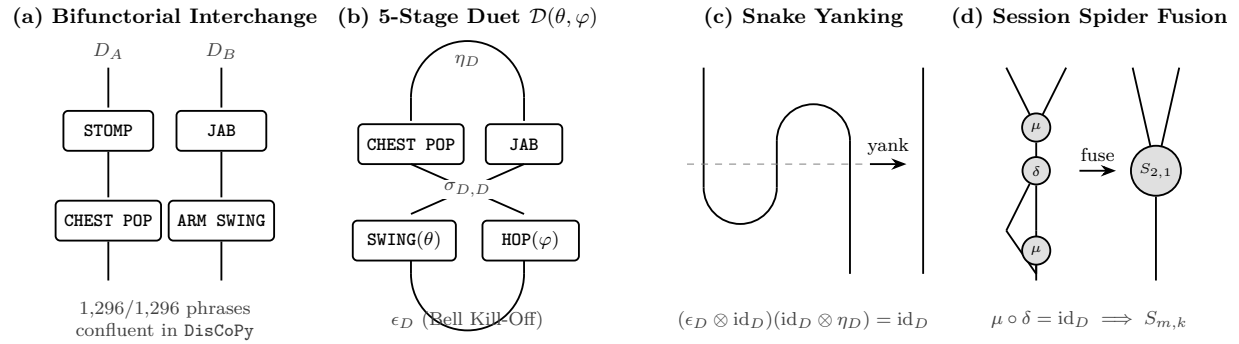


Figure 1: String diagrams in $\mathcal{C}_{\text{Krump}}(\Theta)$ (time flows top-to-bottom): (a) Bifunctorial interchange verified across all 1,296 two-step phrases; (b) Five-stage Effort-parameterized entangled duet $\mathcal{D}(\theta,\varphi)$; (c) Topological snake yanking across a $D^{\otimes 3}$ slice; (d) Special commutative †-Frobenius session-hype spider fusion.

4 Hilbert Semantics and Dual-Channel Non-Clifford Effort Demultiplexing

4.1 Strict Orthonormal Spiders vs. Projective Unit-Norm Quantum Circuits

A frequent source of confusion in categorical quantum mechanics is the scalar factor $\sqrt{2}$ separating unnormalized Z-spiders from physical unit-norm Bell state preparations. We resolve both interpretations explicitly via two related functors.

Theorem 4.1 (Strict **FHilb** Realization vs. Projective Circuit Semantics)**.** *Define the assignment* $\mathcal{F}^{\text{strict}}_{\theta,\varphi} : \mathcal{C}_{\text{Krump}}(\Theta) \to \mathbf{FHilb}$ *on object* $D \mapsto \mathbb{C}^2$ *by Table 1 on movement boxes (*`STOMP` $\mapsto H$, `JAB` $\mapsto X$, `CHEST POP` $\mapsto Z$, `ARM SWING`$(\theta) \mapsto R_x(\theta)$, `BUCK HOP`$(\varphi) \mapsto R_z(\varphi)$, `KILL-OFF` $\mapsto |0\rangle\langle 0|$*) and on structural Frobenius generators by the standard computational-basis copy/merge operators:*

$$\delta_{\text{raw}} = |00\rangle\langle 0| + |11\rangle\langle 1|, \quad \mu_{\text{raw}} = \delta^\dagger_{\text{raw}}, \quad \iota_{\text{raw}} = |0\rangle + |1\rangle, \quad \zeta_{\text{raw}} = \langle 0| + \langle 1|. \tag{6}$$

Then:

1. $\mathcal{F}^{\text{strict}}_{\theta,\varphi}$ *is a* ***strict*** *symmetric monoidal †-functor on structural diagrams (and strict on the Effort rotation generators modulo the standard spinor phase* $R_x(2\pi) = R_z(2\pi) = -I_2$ *in* $\mathrm{SU}(2)$*, hence strict in* $\mathbf{PFHilb} = \mathbf{FHilb}/\mathbb{C}^\times$*):* $\mu_{\text{raw}}\delta_{\text{raw}} = I_2$, $\mu_{\text{raw}}(\iota_{\text{raw}} \otimes I_2) = I_2$, $(I_2 \otimes \mu_{\text{raw}})(\delta_{\text{raw}} \otimes I_2) = \delta_{\text{raw}}\mu_{\text{raw}}$*, and the induced cap* $\eta_{\text{raw}} = \delta_{\text{raw}}\iota_{\text{raw}} = |00\rangle + |11\rangle$ *and cup* $\epsilon_{\text{raw}} = \langle 00| + \langle 11|$ *satisfy* $(\epsilon_{\text{raw}} \otimes I_2)(I_2 \otimes \eta_{\text{raw}}) = I_2$ *with zero scalar defect.*

2. *Physical quantum circuit compilation* $\mathcal{F}^{\text{circ}}_{\theta,\varphi}$ *replaces* $\eta_{\text{raw}}, \epsilon_{\text{raw}}$ *with unit-norm Bell preparation* $\hat{\eta} = \frac{1}{\sqrt{2}}(|00\rangle + |11\rangle) = \mathrm{CX}(H \otimes I_2)|00\rangle$ *and post-selected Bell bra* $\hat{\epsilon} = \hat{\eta}^\dagger = \frac{1}{\sqrt{2}}(\langle 00| + \langle 11|)$*. Consequently,* $(\hat{\epsilon} \otimes I_2)(I_2 \otimes \hat{\eta}) = \frac{1}{2}I_2$ *(encoding the* $1/4$ *post-selection probability of teleportation without classical Pauli feedforward), and the quotient composites* $Q \circ \mathcal{F}^{\text{strict}}_{\theta,\varphi} = Q \circ \mathcal{F}^{\text{circ}}_{\theta,\varphi} : \mathcal{C}_{\text{Krump}}(\Theta) \to \mathbf{PFHilb}$ *coincide identically.*

Proof. Direct matrix multiplication gives $\mu_{\text{raw}}\delta_{\text{raw}} = (|0\rangle\langle 00| + |1\rangle\langle 11|)(|00\rangle\langle 0| + |11\rangle\langle 1|) = |0\rangle\langle 0| + |1\rangle\langle 1| = I_2$, $\mu_{\text{raw}}(\iota_{\text{raw}} \otimes I_2) = (|0\rangle\langle 00| + |1\rangle\langle 11|)(|0\rangle \otimes I_2 + |1\rangle \otimes I_2) = |0\rangle\langle 0| + |1\rangle\langle 1| = I_2$, and $(\epsilon_{\text{raw}} \otimes I_2)(I_2 \otimes \eta_{\text{raw}}) = \sum_{i,j\in\{0,1\}} \langle i|j\rangle\, |i\rangle\langle j| = I_2$. Since $\hat{\eta} = 2^{-1/2}\eta_{\text{raw}}$ and $\hat{\epsilon} = 2^{-1/2}\epsilon_{\text{raw}}$ differ from (6) strictly by non-zero scalars in $\mathbb{C}^\times$, their images in $\mathbf{PFHilb} = \mathbf{FHilb}/\mathbb{C}^\times$ are identical on all morphisms with non-zero contraction. □

4.2 Main Theorem: Dual-Channel Non-Clifford Effort Demultiplexing

In earlier hardware demonstrations [17], fixing Effort angles inside the discrete two-qubit Clifford group ($\theta, \varphi \in \{0, \pi/2, \pi\}$) yielded stabilizer permutations efficiently simulable via the Gottesman–Knill theorem. We now analyze the *full continuous five-stage entangled duet* $\mathcal{D}(\theta, \varphi)$ across arbitrary non-Clifford Laban Effort angles $(\theta, \varphi) \in [0, 2\pi)^2$ (Figure 1b), where Stage 5 applies the complete unitary Bell analyzer $U_{\text{Bell}} = (H \otimes I_2)\,\text{CX}$ followed by computational-basis readout $(m_0, m_1) \in \{0, 1\}^2$.

Lemma 4.2 (Antisymmetric Singlet Ricochet Identity)**.** *Let* $|\Psi^-\rangle = \frac{1}{\sqrt{2}}(|01\rangle - |10\rangle)$ *be the two-qubit singlet state. For any single-qubit operators* $A, B \in \text{SU}(2)$*,*

$$(A \otimes B)\,|\Psi^-\rangle = \big(I_2 \otimes (BYA^\top Y)\big)\,|\Psi^-\rangle, \tag{7}$$

where $Y = \left(\begin{smallmatrix} 0 & -i \\ i & 0 \end{smallmatrix}\right)$*. In particular,* $|\Psi_4(\theta, \varphi)\rangle := (R_x(\theta) \otimes R_z(\varphi))(-|\Psi^-\rangle)$ *satisfies* $\text{Tr}_B(|\Psi_4\rangle\langle\Psi_4|) = \text{Tr}_A(|\Psi_4\rangle\langle\Psi_4|) = \frac{1}{2} I_2$ *and Wootters concurrence* $\mathcal{C}(|\Psi_4(\theta, \varphi)\rangle) = 1$ *for all* $(\theta, \varphi) \in [0, 2\pi)^2$*.*

Proof. Observe that $|\Psi^-\rangle = (I_2 \otimes (-iY))|\Phi^+\rangle$ where $|\Phi^+\rangle = \frac{1}{\sqrt{2}}(|00\rangle + |11\rangle)$. Using the standard cap-ricochet identity $(A \otimes I_2)|\Phi^+\rangle = (I_2 \otimes A^\top)|\Phi^+\rangle$ together with $Y^2 = I_2$, we obtain

$$(A \otimes B)|\Psi^-\rangle = (A \otimes (-iBY))|\Phi^+\rangle = (I_2 \otimes (-iBYA^\top))|\Phi^+\rangle = (I_2 \otimes BYA^\top Y)(I_2 \otimes (-iY))|\Phi^+\rangle,$$

establishing (7). Because $U_{\text{eff}}(\theta, \varphi) := R_z(\varphi) Y R_x(\theta)^\top Y \in \text{SU}(2)$ is unitary, $|\Psi_4(\theta, \varphi)\rangle = (I_2 \otimes U_{\text{eff}})(-|\Psi^-\rangle)$ has Schmidt coefficients $(1/\sqrt{2}, 1/\sqrt{2})$, giving $\rho_A = \rho_B = \frac{1}{2} I_2$ and $\mathcal{C} = 1$. □

Theorem 4.3 (Dual-Channel Effort Demultiplexing and Additive Stabilizer Magic)**.** *Consider the five-stage Effort-parameterized duet circuit compiled from* $\mathcal{C}_{\text{Krump}}(\Theta)$*:*

$$|\Psi_5(\theta, \varphi)\rangle = \underbrace{(H \otimes I_2)\,\text{CX}}_{\text{Stage 5: } \epsilon_D \text{ analyzer}} \quad \underbrace{\big(R_x(\theta) \otimes R_z(\varphi)\big)}_{\text{Stage 4: Effort modulation}} \quad \underbrace{\text{SWAP}}_{\text{Stage 3: } \sigma_{D,D}} \quad \underbrace{(Z \otimes X)}_{\text{Stage 2: POP} \otimes \text{JAB}} \quad \underbrace{\text{CX}\,(H \otimes I_2)|00\rangle}_{\text{Stage 1: } \eta_D}. \tag{8}$$

For all Effort parameters $(\theta, \varphi) \in [0, 2\pi)^2$*:*

1. ***Zero Local Observability Prior to*** ϵ_D***:*** *Any single-dancer local measurement on* $|\Psi_4(\theta, \varphi)\rangle$ *yields uniform random bits* $(1/2, 1/2)$ *with identically zero Classical and Quantum Fisher Information with respect to* (θ, φ)*.*

2. ***Additive Non-Clifford Stabilizer*** 2***-Rényi Magic:*** *The Stabilizer* 2*-Rényi Entropy* $M_2(|\psi\rangle) = -\log_2\big(\frac{1}{4}\sum_{P \in \{I,X,Y,Z\}^{\otimes 2}} |\langle\psi|P|\psi\rangle|^4\big)$ *[20] of the pre-measurement duet state decomposes additively across the two dancers:*

$$M_2\big(|\Psi_4(\theta, \varphi)\rangle\big) = -\log_2\left(1 - \frac{1}{4}\sin^2(2\theta)\right) - \log_2\left(1 - \frac{1}{4}\sin^2(2\varphi)\right). \tag{9}$$

   Thus $M_2(\theta, \varphi) = 0$ *if and only if* $(\theta, \varphi) \in (\frac{\pi}{2}\mathbb{Z})^2$ *(the discrete Clifford studio anchors), and* M_2 *attains its global maximum* $2\log_2(4/3) = \log_2(16/9) \approx 0.830075$ *bits at the non-Clifford quarter-turn Effort modulations* $\theta, \varphi \in \frac{\pi}{4} + \frac{\pi}{2}\mathbb{Z}$*.*

3. ***Exact Product-Channel Demultiplexing at the Climax Cup*** ϵ_D***:*** *Measuring* $|\Psi_5(\theta, \varphi)\rangle$ *in the computational basis* $\{|m_0 m_1\rangle\}_{m_0, m_1 \in \{0,1\}}$ *produces the exact factored Born distribution*

$$\begin{aligned} P(00 \mid \theta, \varphi) &= \sin^2\frac{\varphi}{2}\,\sin^2\frac{\theta}{2}, & P(01 \mid \theta, \varphi) &= \sin^2\frac{\varphi}{2}\,\cos^2\frac{\theta}{2}, \\ P(10 \mid \theta, \varphi) &= \cos^2\frac{\varphi}{2}\,\sin^2\frac{\theta}{2}, & P(11 \mid \theta, \varphi) &= \cos^2\frac{\varphi}{2}\,\cos^2\frac{\theta}{2}, \end{aligned} \tag{10}$$

   routing Dancer B's phase rebound φ *cleanly onto marginal bit* m_0 $(P(m_0 = 0) = \sin^2(\varphi/2))$ *and Dancer A's rotational sweep* θ *cleanly onto marginal bit* m_1 $(P(m_1 = 0) = \sin^2(\theta/2))$*.*

4. ***Simultaneous Multiparameter Quantum Cramér–Rao Saturation:*** *For all* $(\theta, \varphi) \notin (\pi\mathbb{Z})^2$*, the* 2×2 *Classical Fisher Information matrix of the single fixed Bell readout* (10) *is diagonal and constant, saturating the multiparameter Quantum Fisher Information matrix:*

$$I_C(\theta, \varphi) = I_Q\big(|\Psi_4(\theta, \varphi)\rangle\big) = \begin{pmatrix} 1 & 0 \\ 0 & 1 \end{pmatrix}. \tag{11}$$

Proof. Stages 1–3 evaluate directly on $|00\rangle$:

$$\mathrm{CX}(H \otimes I_2)|00\rangle = \frac{|00\rangle + |11\rangle}{\sqrt{2}} \overset{Z\otimes X}{\longmapsto} \frac{|01\rangle - |10\rangle}{\sqrt{2}} \overset{\text{SWAP}}{\longmapsto} \frac{|10\rangle - |01\rangle}{\sqrt{2}} = -|\Psi^-\rangle.$$

Part (1) then follows immediately from Lemma 4.2, since $\rho_A(\theta, \varphi) = \rho_B(\theta, \varphi) = \frac{1}{2} I_2$ is independent of (θ, φ).

For Part (2), since $-|\Psi^-\rangle$ has stabilizer generators $\langle -X \otimes X, -Y \otimes Y, -Z \otimes Z\rangle$, conjugating the 16 two-qubit Pauli operators by $R_x(\theta) \otimes R_z(\varphi)$ leaves all 6 single-qubit marginals and $X \otimes Z$ with expectation 0, while the 9 non-vanishing expectations are:

$$\begin{aligned} &\langle I \otimes I\rangle = 1, \quad \langle X \otimes X\rangle = -\cos\varphi, \quad \langle X \otimes Y\rangle = -\sin\varphi, \\ &\langle Z \otimes Z\rangle = -\cos\theta, \quad \langle Y \otimes Z\rangle = \sin\theta, \quad \langle Y \otimes X\rangle = \cos\theta\sin\varphi, \\ &\langle Y \otimes Y\rangle = -\cos\theta\cos\varphi, \quad \langle Z \otimes X\rangle = \sin\theta\sin\varphi, \quad \langle Z \otimes Y\rangle = -\sin\theta\cos\varphi. \end{aligned}$$

Summing their fourth powers factors algebraically as a product:

$$\frac{1}{4}\sum_{P \in \mathcal{P}_2} \langle P\rangle^4 = \frac{1 + \cos^4\theta + \sin^4\theta}{2} \cdot \frac{1 + \cos^4\varphi + \sin^4\varphi}{2} = \left(1 - \frac{1}{4}\sin^2(2\theta)\right)\left(1 - \frac{1}{4}\sin^2(2\varphi)\right),$$

using $\cos^4\alpha + \sin^4\alpha = 1 - \frac{1}{2}\sin^2(2\alpha)$. Taking $-\log_2$ yields (9). Since $\sin^2(2\alpha) \in [0, 1]$, each term lies in $[0, \log_2(4/3)]$, vanishing iff $\sin(2\alpha) = 0 \iff \alpha \in \frac{\pi}{2}\mathbb{Z}$ and peaking at $\sin^2(2\alpha) = 1 \iff \alpha \in \frac{\pi}{4} + \frac{\pi}{2}\mathbb{Z}$.

For Part (3), write $R_x(\theta) = \cos\frac{\theta}{2} I_2 - i\sin\frac{\theta}{2} X$ and $R_z(\varphi) = \cos\frac{\varphi}{2} I_2 - i\sin\frac{\varphi}{2} Z$. Acting on $-|\Psi^-\rangle$ expands $|\Psi_4(\theta, \varphi)\rangle$ cleanly across the four Bell states $|\Phi^\pm\rangle = \frac{|00\rangle \pm |11\rangle}{\sqrt{2}}$, $|\Psi^\pm\rangle = \frac{|01\rangle \pm |10\rangle}{\sqrt{2}}$:

$$|\Psi_4(\theta, \varphi)\rangle = -\cos\frac{\theta}{2}\cos\frac{\varphi}{2}|\Psi^-\rangle + i\cos\frac{\theta}{2}\sin\frac{\varphi}{2}|\Psi^+\rangle + i\sin\frac{\theta}{2}\cos\frac{\varphi}{2}|\Phi^-\rangle + \sin\frac{\theta}{2}\sin\frac{\varphi}{2}|\Phi^+\rangle. \tag{12}$$

Because $U_{\text{Bell}} = (H \otimes I_2)\,\mathrm{CX}$ maps $|\Phi^+\rangle \mapsto |00\rangle$, $|\Psi^+\rangle \mapsto |01\rangle$, $|\Phi^-\rangle \mapsto |10\rangle$, and $|\Psi^-\rangle \mapsto -|11\rangle$, taking squared moduli of (12) yields (10) directly.

Finally, for Part (4), since $P(m_0, m_1 \mid \theta, \varphi) = p_\varphi(m_0)\, p_\theta(m_1)$ is a product of single-parameter Bernoulli distributions depending solely on φ and θ respectively, off-diagonal Classical Fisher Information vanishes ($I_{C,\theta\varphi} = 0$), while $I_{C,\theta\theta} = \frac{[\partial_\theta(\sin^2(\theta/2))]^2}{\sin^2(\theta/2)\cos^2(\theta/2)} = \frac{(\frac{1}{2}\sin\theta)^2}{\frac{1}{4}\sin^2\theta} = 1$ and identically $I_{C,\varphi\varphi} = 1$. Since $|\Psi_4(\theta, \varphi)\rangle$ is generated from a fixed state by commuting generators $G_\theta = \frac{1}{2}(X \otimes I_2)$ and $G_\varphi = \frac{1}{2}(I_2 \otimes Z)$ with zero expectation and unit variance ($\langle G_\theta^2\rangle = \langle G_\varphi^2\rangle = 1/4$, $\langle G_\theta G_\varphi\rangle = \frac{1}{4}\langle X \otimes Z\rangle = 0$), $I_Q = 4\,\mathrm{Cov}(G_\theta, G_\varphi) = \mathrm{diag}(1, 1)$, proving (11). □

Remark 4.4 (Choreographic Meaning of Theorem 4.3)**.** Theorem 4.3 captures a striking formal duality: while the duet is in progress (Stage 4), observing either dancer in isolation reveals nothing about either dancer's continuous Effort intensity ($\rho_A = \rho_B = \frac{1}{2} I_2$), yet closing the phrase with the synchronized joint kill-off (ϵ_D) simultaneously decodes *both* dancers' continuous Effort angles without cross-talk, even in the maximally non-Clifford regime ($\theta = \varphi = \pi/4$, $M_2 = \log_2(16/9)$ bits; Figure 2). Moreover, setting $(\theta, \varphi) \in \{0, \pi\}^2$ recovers deterministic superdense coding of all four 2-bit battle outcomes $\{00, 01, 10, 11\}$.

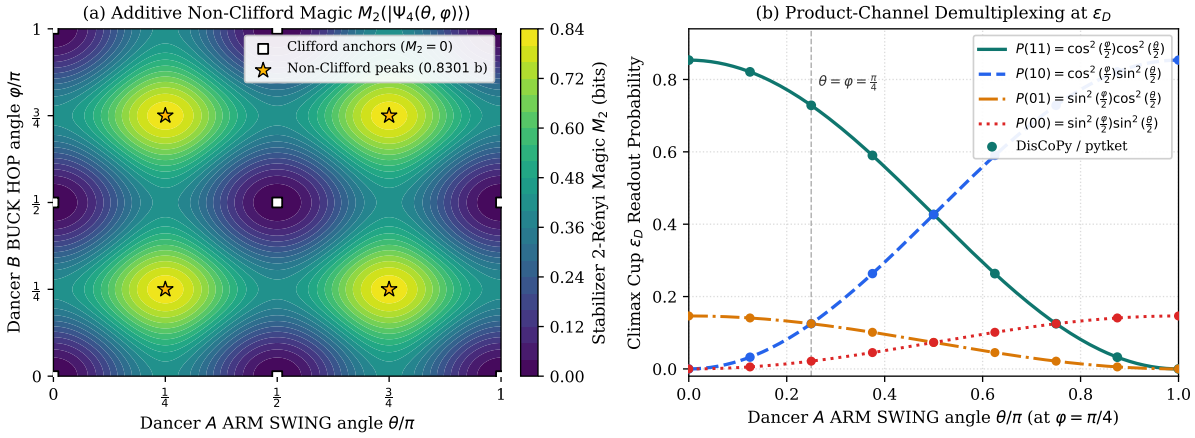


Figure 2: Analytical and numerical verification of Theorem 4.3: (a) Two-dimensional landscape of additive Stabilizer 2-Rényi Magic $M_2(|\Psi_4(\theta,\varphi)\rangle)$, contrasting discrete Clifford anchors ($M_2 = 0$, white squares) with quarter-turn non-Clifford Effort peaks ($M_2 = \log_2(16/9) \approx 0.8301$ bits, gold stars); (b) Exact product-channel Born probabilities at the climax cup ϵ_D along $\varphi = \pi/4$, overlaid with `DisCoPy 1.2.2` and `pytket 2.18.1` evaluations.

5 Planar Stage Realizability of Symmetric Crossovers $\sigma_{D,D}$

In the abstract symmetric monoidal category $\mathcal{C}_{\text{Krump}}(\Theta)$, wire permutation $\sigma_{D,D} : D \otimes D \to D \otimes D$ is a primitive generator. On a physical two-dimensional stage, however, two dancers cannot pass through the same floor coordinate or swap positions head-on across a narrow corridor at the same beat. We link $\sigma_{D,D}$ to discrete spatial geometry via exact binary polynomial quadratization.

Proposition 5.1 (Exact Rosenberg Quadratization for Collision- and Swap-Free Stage Braiding)**.** *Let $G_{\text{stage}} = (V_S, E_S)$ be a finite undirected graph representing stage zones, $T = \{0, 1, \ldots, \tau\}$ be discrete beat steps, and $x_{a,v,t} \in \{0,1\}$ indicate whether dancer $a \in \{1, \ldots, n\}$ occupies vertex $v \in V_S$ at beat $t \in T$. Enforcing (i) unique occupancy $\sum_{v \in V_S} x_{a,v,t} = 1$, (ii) kinematic adjacency $x_{a,u,t} x_{a,v,t+1} = 0$ for $\{u, v\} \notin E_S \cup \{\{v, v\}\}$, (iii) no vertex collisions $x_{a,v,t} x_{b,v,t} = 0$ $(a < b)$, and (iv) no simultaneous head-on edge swaps across any $\{u, v\} \in E_S$:*

$$H_{\text{swap}} = \lambda_{\text{swap}} \sum_{t=0}^{\tau-1} \sum_{a<b} \sum_{\{u,v\} \in E_S} \left(x_{a,u,t}\, x_{a,v,t+1}\, x_{b,v,t}\, x_{b,u,t+1} + x_{a,v,t}\, x_{a,u,t+1}\, x_{b,u,t}\, x_{b,v,t+1} \right) \tag{13}$$

defines a degree-4 Higher-Order Unconstrained Binary Optimization (HUBO) problem realizing a target permutation $\pi \in S_n$ ($x_{a,v_{\text{init}}(a),0} = x_{a,v_{\text{init}}(\pi(a)),\tau} = 1$). Introducing auxiliary binary variables $y^+_{a,t,e}, y^-_{a,t,e} \in \{0,1\}$ for directed edge traversals $(u \to v)$ and $(v \to u)$ with Rosenberg penalty [21]

$$R_M(x_1, x_2, y) = M\,(x_1 x_2 - 2x_1 y - 2x_2 y + 3y), \qquad M > \lambda_{\text{swap}} + \max|H_{\text{stage}}|, \tag{14}$$

reduces (13) to a strictly quadratic QUBO $\widetilde{H}(x, y)$ whose global minima project bijectively onto the collision- and swap-free global minima of the original HUBO.

Proof. For binary $(x_1, x_2, y) \in \{0,1\}^3$, examine $g(x_1, x_2, y) := x_1 x_2 - 2x_1 y - 2x_2 y + 3y$: when $y = x_1 x_2$, $g(x_1, x_2, x_1 x_2) = x_1 x_2 - 4x_1 x_2 + 3x_1 x_2 = 0$ for all four pairs $(x_1, x_2) \in \{0,1\}^2$. Conversely, if $y \neq x_1 x_2$, either $(x_1, x_2) = (1,1), y = 0 \implies g = 1 \geq 1$, or $x_1 x_2 = 0, y = 1 \implies g = 3 - 2(x_1 + x_2) \geq 1$ since $x_1 + x_2 \leq 1$. Thus $R_M(x_1, x_2, y) = 0$ iff $y = x_1 x_2$ and $R_M \geq M$ otherwise. Substituting $y^+_{a,t,e} = x_{a,u,t} x_{a,v,t+1}$ and $y^-_{b,t,e} = x_{b,v,t} x_{b,u,t+1}$ converts each quartic monomial in (13) into the quadratic product $\lambda_{\text{swap}}\, y^+_{a,t,e} y^-_{b,t,e}$ while preserving exact ground states for $M > \lambda_{\text{swap}} + \max|H_{\text{stage}}|$. □

6 Multi-Backend Verification and Classical Contraction Floors

Every algebraic identity, symbolic Born distribution, magic decomposition, and native trapped-ion compilation metric established in Sections 2–5 is checked by a deterministic, zero-parameter script (`verify_categorical_choreography_theorems.py`) executing upstream `DisCoPy 1.2.2`, `SymPy 1.14.0`, `pytket 2.18.1`, and `NumPy 2.5.2` (Table 3).

Table 3: Summary of deterministic symbolic, tensor-network, compiler, and trapped-ion emulator verifications for CatKS and $\mathcal{C}_{\text{Krump}}(\Theta)$.

Result / Theorem	**Verification Engine**	**Quantitative Metric**	**Verified Outcome**
Theorem 2.4 (Yoneda Profiles)	`NumPy 2.5.2` (A_G^k)	6/6 distinct columns	Exact $M_{\leq 4}$ path counts; 11 paths into `CHEST POP`.
Theorem 3.2(1) (Interchange)	`DisCoPy 1.2.2`	1,296/1,296 tuples	Exhaustive 2-step duet `normal_form()` confluence.
Theorem 3.2(2–4) (Coherence)	`DisCoPy 1.2.2`	Hypergraph exact	Left/right snakes, $\sigma^2 = \text{id}$, 3-strand Yang–Baxter, $S_{m,k}$.
Theorem 4.1 (Strict **FHilb**)	`NumPy 2.5.2`	$\|\Delta\|_2 = 0.0$	Exact special commutative †-Frobenius & snake matrices.
Lemma 4.2 (Singlet Ricochet)	`NumPy 2.5.2`	$\|\Delta\|_2 = 0.0$	$\mathcal{C}(\theta, \varphi) = 1.000000$ across all 625 (θ, φ) grid points.
Theorem 4.3 (Demultiplexing)	`SymPy` + `DisCoPy` + `pytket`	$\max \|\Delta\|_2 = 2.1 \times 10^{-8}$	Exact product Born law (10) across 25×25 Effort grid.
Theorem 4.3(2) (Stabilizer Magic)	`SymPy` + Pauli $\mathcal{P}_2$	$M_2(\frac{\pi}{4}, \frac{\pi}{4}) = 0.830075$ b	Vanishes at Clifford $(\frac{\pi}{2}, \frac{\pi}{2})$; peaks at $\log_2(16/9)$ bits.
Native Ion Compilation	`pytket 2.18.1` `AutoRebase`	$F = 1 - 4 \times 10^{-16}$	Full 5-stage non-Clifford duet $\mapsto$ 5 `ZZPhase` + 14 `PhasedX`.
Noisy Trapped-Ion Emulator	Quantinuum `Helios-1E-lite`	99.41% (1,018/1,024)	Clifford-anchor duet Job `a411dac7`; ladder $R^2 = 0.9942$ (`d43f26d9`).
Proposition 5.1 (Stage QUBO)	OpenJij SA (348 vars)	$E_0 = -7.3569$	0 vertex collisions, 0 midpoint swaps on 5×4 stage grid.
Classical CPU Floor	Single-core `NumPy`	0.63 μs (2q) / 1.74 μs (4q)	Explicit classical baseline (0 physical QPU shots claimed).

Cross-Checking DisCoPy, SymPy, pytket, and Quantinuum Native Compilation. Across a uniform 25×25 grid (625 points) spanning $(\theta, \varphi) \in [0, 2\pi)^2$, statevectors evaluated via `DisCoPy` circuit contraction ($\texttt{Rx}(\theta/2\pi) \otimes \texttt{Rz}(\varphi/2\pi)$) and `pytket` unitary simulation ($\texttt{Rx}(\theta/\pi) \otimes \texttt{Rz}(\varphi/\pi)$) match the closed-form analytical expansion (12) within floating-point precision ($\max \|\Delta\|_2 = 2.11 \times 10^{-8}$, arising solely from single-precision phase serialization inside circuit boxes). At the non-Clifford quarter-turn Effort modulation $(\theta, \varphi) = (\pi/4, \pi/4)$, the Bell-analyzer Born probabilities evaluate to

$$P(00) = \sin^4 \frac{\pi}{8} \approx 0.021447, \quad P(01) = P(10) = \frac{1}{8} = 0.125000, \quad P(11) = \cos^4 \frac{\pi}{8} \approx 0.728553, \tag{15}$$

with exact Stabilizer 2-Rényi Magic $M_2(\pi/4, \pi/4) = \log_2(16/9) = 0.830075$ bits. Compiling the un-elided 5-stage non-Clifford circuit (retaining explicit 3-`CX` stage swap $\sigma_{D,D}$) via `pytket`'s `AutoRebase` into Quantinuum's native trapped-ion gate set $\{\texttt{ZZPhase}, \texttt{PhasedX}, \texttt{Rz}\}$ produces exactly 5 two-qubit `ZZPhase` gates, 14 single-qubit `PhasedX` pulses, and 14 virtual `Rz` frame updates at statevector fidelity $F = 0.9999999999999996$. On Quantinuum's noise-modeled `Helios-1E-lite` trapped-ion emulator (`alpha` noise model, Guppy 1.0 $\rightarrow$ HUGR; 0 physical QPU shots claimed), the 5-stage Clifford-anchor projection executed at 1,018/1,024 = 99.41% readout fidelity (Job `a411dac7`), complemented by an 8-rung single-qubit phase/colatitude ladder achieving $R^2 = 0.9942$ ($a = 0.4926 \pm 0.0076$, $b = 0.4891 \pm 0.0215$; Job `d43f26d9`). Meanwhile, exact single-core CPU matrix-vector evaluation of the 2-qubit duet requires $0.63\,\mu$s ($1.74\,\mu$s at 4 qubits), underscoring that finite-width choreographic compilation is a compositional semantics contribution rather than a claim of quantum computational supremacy.

7 Conclusion

By lifting solo Krump posture quivers (CatKS) into a parameterized symmetric monoidal †-compact Frobenius category ($\mathcal{C}_{\text{Krump}}(\Theta)$), we obtain an exact, machine-verified graphical calculus for concurrent multi-dancer street dance choreography. Beyond syntactic coherence (interchange, snake yanking, Yang–Baxter crossovers, and Frobenius session-hype fusion), interpreting $\mathcal{C}_{\text{Krump}}(\Theta)$ in **FHilb** uncovers a sharp analytical phenomenon—the *Dual-Channel Effort Demultiplexing Theorem*—in which locally unobservable, maximally entangled, non-Clifford Effort modulations ($M_2 \leq \log_2(16/9)$ bits) separate into independent, Cramér–Rao-optimal classical readout channels upon closing the duet with a synchronized climax cup ϵ_D. Together with exact Rosenberg quadratization for planar stage routing, this work places urban movement practice alongside natural language and musical counterpoint inside modern applied category theory.

Data and Code Availability

Open-source verification scripts (`experiments/verify_categorical_choreography_theorems.py` and `experiments/discopy_krump_string_diagrams.py`), JSON receipts, and ontology specifications are archived at https://arunnadarasa.github.io/quantumkrump/.

Acknowledgments

This work was supported in part by complimentary access to Google Antigravity and Gemini 4 Argon to accelerate scientific workflows. We gratefully acknowledge the Quantinuum Bradford Hackathon 2025, UNESCO IYQ 2025, Quantinuum (`DisCoPy`, `pytket`, and Nexus `Helios-1E-lite`), OpenJij, and the South Central LA, European, and Indian Krump communities, including mentors Prince Yarjack (Asura), Yarjack (Easy / Easyar Dojo), Hectik (Jr Asura), Kronos (Lil Asura), IKF, AKF, and Point Blank Fam.

AI Use Declaration

Large language models including Gemini 4 Argon, accessed within Google Antigravity, were used during this project to assist with symbolic verification scripts, visualization code, manuscript editing, and adversarial review diagnostics. Throughout all stages, the authors directed the mathematical formulation, verified every proof, symbolic identity, compiler output, figure, and bibliographic citation against primary sources and deterministic execution receipts, and take full responsibility for all analyses, claims, and content in this manuscript.

References

[1] Bob Coecke, Mehrnoosh Sadrzadeh, and Stephen Clark. Mathematical foundations for a compositional distributional model of meaning. In *Lambek Festschrift, Linguistic Analysis*, volume 36, pages 345–384. 2010.

[2] Guerino Mazzola and Maria Mannone. Global functorial hypergestures over general skeleta for musical performance. *Journal of Mathematics and Music*, 10(2):93–106, 2016.

[3] Moreno Andreatta, Andrée C. Ehresmann, René Guitart, and Guerino Mazzola. Towards a categorical theory of creativity for music, discourse, and cognition. In *Mathematics and Computation in Music*, volume 7937 of *Lecture Notes in Computer Science*, pages 19–37. Springer, Berlin, Heidelberg, 2013.

[4] Ilyas Khan. Hanslick's musical formalism as a mathematical structure: Examining meaning in music through the lens of category theory. *arXiv preprint arXiv:2610.17388*, 2026.

[5] Rakhat-Bi Abdyssagin and Bob Coecke. Quantum concept music score from quantum picturalism: Musical incarnation of a Bell-pair under measurements. *arXiv preprint arXiv:2510.05391*, 2025.

[6] Maria Mannone. Introduction to gestural similarity in music: An application of category theory to the orchestra. *arXiv preprint arXiv:1904.10340*, 2019.

[7] Maria Mannone and Luca Turchet. Shall we (math and) dance? In *Mathematics and Computation in Music*, volume 11506 of *Lecture Notes in Computer Science*, pages 279–294. Springer, Cham, 2019.

[8] Brendan Fong and David I. Spivak. *An Invitation to Applied Category Theory: Seven Sketches in Compositionality*. Cambridge University Press, Cambridge, UK, 2019.

[9] Tommaso Salvatori, Matteo Forasassi, Alexis Toumi, and Giovanni de Felice. Tiny recursive message passing. *arXiv preprint arXiv:2610.18649*, 2026.

[10] André Joyal and Ross Street. The geometry of tensor calculus, I. *Advances in Mathematics*, 88(1):55–112, 1991.

[11] Peter Selinger. Dagger compact closed categories and completely positive maps. *Electronic Notes in Theoretical Computer Science*, 170:139–163, 2007.

[12] Bob Coecke and Ross Duncan. Interacting quantum observables. In *Automata, Languages and Programming (ICALP 2008)*, volume 5126 of *Lecture Notes in Computer Science*, pages 298–310. Springer, 2008.

[13] Bob Coecke and Aleks Kissinger. *Picturing Quantum Processes: A First Course in Quantum Theory and Diagrammatic Reasoning*. Cambridge University Press, Cambridge, UK, 2017.

[14] David LaChapelle. *Rize*. Documentary film, Lions Gate Entertainment, 2005.

[15] Rudolf Laban and F. C. Lawrence. *Effort: Economy of Human Movement*. Macdonald & Evans, London, 1947.

[16] Andreas Aristidou, Panayiotis Charalambous, and Yiorgos Chrysanthou. Emotion analysis and classification: Understanding the performers' emotions using the LMA entities. *Computer Graphics Forum*, 34(6):262–276, 2015.

[17] Arun Nadarasa and Dakota Simao. Embodied quantum pedagogy through Krump street dance, Laban movement analysis, and string diagrams. Open-access companion preprint, https://arunnadarasa.github.io/quantumkrump/downloads/quantum-krump-pedagogy-paper.pdf, 2026.

[18] Arun Nadarasa. KrumpRobot: High-jerk expressive humanoid dance generation via monocular 3d motion recovery, rest-relative retargeting, and phase-conditioned neural control. Open-access companion preprint, https://arunnadarasa.github.io/quantumkrump/downloads/krumprobot-physical-ai-paper.pdf, 2026.

[19] Giovanni de Felice, Alexis Toumi, and Bob Coecke. DisCoPy: Monoidal categories in Python. In *Proceedings of Applied Category Theory 2020 (ACT 2020)*, volume 333 of *Electronic Proceedings in Theoretical Computer Science (EPTCS)*, pages 83–97, 2020.

[20] Lorenzo Leone, Salvatore F. E. Oliviero, and Alioscia Hamma. Stabilizer Rényi entropy. *Physical Review Letters*, 128(5):050402, 2022.

[21] Ivo G. Rosenberg. Reduction of bivalent maximization to the quadratic case. *Cahiers du Centre d'Études de Recherche Opérationnelle*, 17:71–74, 1975.

[22] Seyon Sivarajah, Silas Dilkes, Alexander Cowtan, Will Simmons, Alec Edgington, and Ross Duncan. t|ket⟩: A retargetable compiler for NISQ devices. *Quantum Science and Technology*, 6(1):014003, 2020.

[23] Eduard Hanslick. *On the Musically Beautiful: A Contribution towards the Revision of the Aesthetics of Music*. Hackett Publishing, Indianapolis, IN, 1986. Original work published 1854.

[24] Saunders Mac Lane. *Categories for the Working Mathematician*, volume 5 of *Graduate Texts in Mathematics*. Springer, New York, 2nd edition, 1998.